Earthq Eng & Eng Vib (2024) 23: 563-576 **DOI**: https://10.1007/s11803-024-2257-5

Single-station microtremor surveys for site characterization: A case study in Erzurum city, eastern Turkey

Fatih Karsli[1†] and Erdem Bayrak[2, 3‡]

1. *The Higher Education Credit and Hostels Institution, Ministry of Youth and Sports, Erzurum 25240, Turkey*
2. *Earthquake Research Centre, Ataturk University, Erzurum 25240, Turkey*
3. *Department of Civil Engineering, Ataturk University, Erzurum 25240, Turkey*

Abstract: The single-station microtremor method is one of the fastest, most reliable, and cheapest methods used to identify dynamic soil properties. This study utilizes 49 single-station microtremor measurements to identify the dynamic soil properties of the Hilalkent quarter of the Yakutiye district in Erzurum. Soil dominant frequency and the amplification factor were calculated by using the Nakamura horizontal/vertical spectral ratio (H/V) method. While the soil dominant frequency values varied between 0.4 Hz and 10 Hz, the soil amplification factor changed between 1 and 10. Higher H/V values were acquired with lower frequency values. The vulnerability index (K_g) and shear strain parameters that are utilized to estimate the damage that may be caused by an earthquake were mapped. Especially in the west side of the study area, higher K_g values were observed. The shear strain map was created with 0.25 g, 0.50 g and 0.75 g bedrock accelerations, and soil types that lost elasticity during an earthquake were identified. The average shear wave velocity for the first 30 m (V_{s30}) was calculated. Finally, it was observed that the western part of the study area, which resulted in a higher period and higher H/V, higher K_g and lower V_{s30} values, presents a higher risk of damage during an earthquake.

Keywords: Nakamura horizontal/vertical spectral ratio; single-station microtremor; predominant frequency; vulnerability index; Erzurum

1 Introduction

An earthquake is one of the most destructive natural disasters that has occurred throughout human history. Turkey is located in the Alpine-Himalayan earthquake belt, which is one of the most active earthquake belts in the world. The incidents that shaped the tectonic characteristics of Turkey include the movements of the Arabian plate towards the north, the African plate to the northeast, the Eurasian plate to the south, and the pressurization of the eastern section of the Anatolian plate. The north Anatolian fault zone (NAFZ) and the east Anatolian fault zone (EAFZ) were created as a result of the relative movements of these plates (Keskin *et al*., 1998). On the other hand, Erzurum is located in the east of Turkey and is 70 km from the Karliova, the triple junction of the east Anatolian and the north Anatolian fault zones. Erzurum experienced many destructive earthquakes in the historical (<1900) and instrumental periods, resulting in numerous instances of significant damage (Soysal *et al*., 1981; Koçyigit and Canoglu, 2017). On February 6, 2023, two earthquakes occurred on the eastern Anatolian fault zone in eastern Turkey, the first with a magnitude of M_w 7.7 in the Pazarcık district and, about nine hours later, the second with a magnitude of M_w 7.6 in the Elbistan district. Erzurum's city center is located about 500 km from the first earthquake and about 400 km from the second. At acceleration stations 2501, 2508 and 2509 in the city center, peak acceleration values of 7 gal, 10 gal and 6 gal were recorded in the first earthquake, and 5 gal, 7 gal and 5 gal in the second. Although serious damage was reported in many cities (Baser *et al*., 2023; Binici *et al*., 2023), no damage was reported in Erzurum from these two earthquakes. In the literature there have been a number of studies conducted specifically in the field of geosciences. The tectonic and geological evolution of Erzurum was discussed by Keskin *et al*. (1998) and Koçyigit and Canoglu (2017). While its geochemical properties were studied by Bayraktutan *et al*. (1996), its geothermal features were assessed by Bektaş *et al*. (2007) and Özer and Ozyazicioglu (2019). Özer (2019), on the other hand, focused on local soil features by utilizing strong ground motion records and observed a higher value of amplification with a lower value of frequency in the stations located on alluvial grounds. Bayrak *et al*. (2020), by using the focal mechanism solutions of earthquakes

Correspondence to: Erdem Bayrak, Earthquake Research Centre, Ataturk University, 25240, Erzurum, Turkey; Department of Civil Engineering, Ataturk University, 25240, Erzurum, Turkey
Tel.: +90-4423165000
Email: erdmbyrk@gmail.com
[†]Engineer MSc; [‡]Assistant Professor
Received January 31, 2023; **Accepted** August 26, 2023

that occurred in Erzurum and its proximity, identified areas with decreased or increased tectonic tensions, while underlining seismic hazards.

The studies conducted to decrease the damage that might be caused by earthquakes are among the most important factors that could mitigate the damage caused to humanity by these natural disasters. Various soil dynamic characteristics present different behaviors as a result of the various dynamic forces created by an earthquake. Accordingly, these different behaviors create diverse effects in damage to different types of buildings. Therefore, identifying soil dynamic properties is of utmost importance for building designs. Evaluating the reactions of buildings and soil against seismic influences is a crucial part of assessing the interaction between earthquakes, soil, and buildings. In particular, identifying the features of surface layers, also known as local soil conditions, will further support estimates regarding an earthquake's effect on a specific building (Nakamura, 1989).

Why buildings constructed on bad or soft ground rather than on strong or solid ground show greater damage during an earthquake can be explained by the amplification of the ground. Kramer (1996) identifies soil amplification as follows: the bedrock records with lower acceleration values, together with the effects of the ground layers, while the acceleration value reaches the surface in some areas and simultaneously expands multiple times, may cause significant and permanent damage to buildings. For the identification of dynamic soil properties, geophysical methods are also actively used in addition to direct identification with drilling or methods of identification conducted in the laboratory (Borcherdt *et al*., 1991; Park *et al*., 1999; Okada and Suto, 2003). Similarly, the single-station microtremor method is often used to identify local soil properties. The horizontal/vertical spectral ratio method (HVSR or H/V) is applied by proportioning the horizontal component Fourier amplitude spectrum of noise records achieved with a three-component seismometer to the vertical component Fourier amplitude spectrum (Molnar *et al*., 2022). Today, the microtremor method is often preferred because of its low cost and rapid measurement features, thus allowing a rapid analysis. The application field of the microtremor method increases with every passing day. Measurements conducted by using the microtremor method also provide important physical parameters regarding soil properties. This method is frequently used in earthquake engineering and seismological studies (Nakamura, 1989; Lermo and Chávez-García, 1993; Field and Jacob, 1995; Konno and Ohmachi, 1998; Kawase *et al*., 2011; Paudyal *et al*., 2012; SESAME, 2004; Wen *et al*., 2011; Akin and Sayil, 2016; Livaoğlu *et al*., 2021; Jirasakjamroonsri *et al*., 2019; Pamuk, 2019; Kanbur *et al*., 2020; Putti and Satyam, 2020; Tallini *et al*., 2020; Akkaya, 2020; Zavala *et al*., 2021; Akbayram *et al*. 2022).

Concerning the scope of this study, the single-station microtremor measurements of 49 locations in the Hilalkent quarter of the Yakutiye district in Erzurum province were utilized to identify the local soil properties of dominant ground frequency and the soil amplification factor. The data were analyzed by using the Nakamura horizontal/vertical spectral ratio method. The vulnerability index (K_g) and the shear strain values which represent the areas that may suffer damage as a result of an earthquake were calculated by using the dominant frequency period and amplification factor values. Additionally, the V_{s30} (the mean value of the shear wave velocity belonging to the layers of the first 30 m of ground) value was also calculated by using the empirical relation method. Finally, these parameters were mapped in order to examine the spatial changes in the soil properties as well as the changes in geological units.

2 Tectonics and geology

Turkey is located in a region with high earthquake potential and has suffered many destructive earthquakes throughout its history, resulting in significant losses of life and property. Statistical earthquake studies in the literature underline the fact that the tectonic structures in and around Turkey have a high potential to produce earthquakes in the future (Erdik *et al*., 1999; Bayrak *et al*., 2009; Bayrak and Bayrak, 2012; Öztürk, 2017; Coban and Sayil, 2019, 2020a, 2020b; Özer *et al*., 2022).

The geological history of the 2.5 to 11 million years of the collision volcanic activity occurring in Erzurum province, located along the Erzurum-Kars Plateau has a unique value (Keskin *et al*., 1998). The disappearance of the Tethys Ocean and the thickening of the earth's crust as a result of the collision of the Arabian and Anatolian plates elevated the region. As a result of the volcanism created by this collision, the Erzurum-Kars Plateau was covered with pyroclastic materials and lava. Volcanic activity that continued for some 2.5-11 million years has increased the thickness of volcanic materials in this plateau to 1 km at certain locations. The volcanic materials often surfaced with strike slip faults that usually intersected the region in the direction of NE-SW and were active during the period of volcanism, filling these basins with lava (Keskin *et al*., 1998; Tavlaşoğlu, 2021). Many cracks or faults, whether small or large, were caused by the continuation of these tectonic movements. They play an important role in the creation of the tectonic structure of Erzurum and its proximity. The most important faults in and around Erzurum can be identified as (Koçyigit and Canoglu, 2017): the Erzurum-Dumlu fault zone (EDFZ), the Palandoken fault zone (PFZ), the Baskoy-Kandilli fault zone (BKFZ) and the Askale Fault Zone (AFZ) (Fig. 1). Additionally, the earthquakes that occurred and have caused damage in Erzurum since 1900 include the 1901 Pasinler-Erzurum (M=6.1), the 1906 Oltu-Erzurum (M= 6.0), 1924 Pasinler (M=6.8) and the 1983 Horasan (M_w=6.6) upheavals (Fig. 1, Table 1).

On the other hand, the earthquakes with magnitudes of 5.6 and 5.5 that occurred in Askale in 2004 also caused life and property loss. On 6 February 2023, two earthquakes of magnitudes 7.7 and 7.6 occurred along the Eastern Anatolia fault zone. Although these earthquakes were felt intensely in Erzurum and its vicinity, they did not cause any damage. As a result of the earthquakes, which affected a large part of Turkey, many researchers evaluated the earthquake from different aspects, including slip distribution and the source model (Li *et al*., 2023; Zhao *et al*., 2023; Melgar *et al*., 2023), strong ground motion parameters (Shao *et al*., 2023; Baltzopoulos *et al*., 2023; Xu *et al*., 2023), magnitude of the earthquake (Jiang *et al*., 2023; Karabulut *et al*., 2023), and damage to structures (Chen *et al*., 2023; Wang *et al*., 2023; Papazafeiropoulos and Plevris, 2023).

Paleo-seismic data indicate that the EFZ produced two late Holocene earthquakes as a result of its northern section moving vertically from 1.5 to 3.0 m. According to these movements and the length of the fault, it is possible that the northern EFZ can produce stronger earthquakes than M_w 7.1, with a return period of 1000 to 3000 years. The close distance of the EFZ to Erzurum province presents a marked degree of danger for the city (Emre *et al*., 2004, 2018).

According to the geomorphology of the study area, the final shape of the region was determined by the plains formed by the elevation of volcanic materials around Erzurum. The plains were also filled by the alluvial materials flowing from the Karasu and Palandoken mountains (Koçyigit and Canoglu, 2017).

The study area usually consists of three different formations (Fig. 2). From the bottom to the top, these

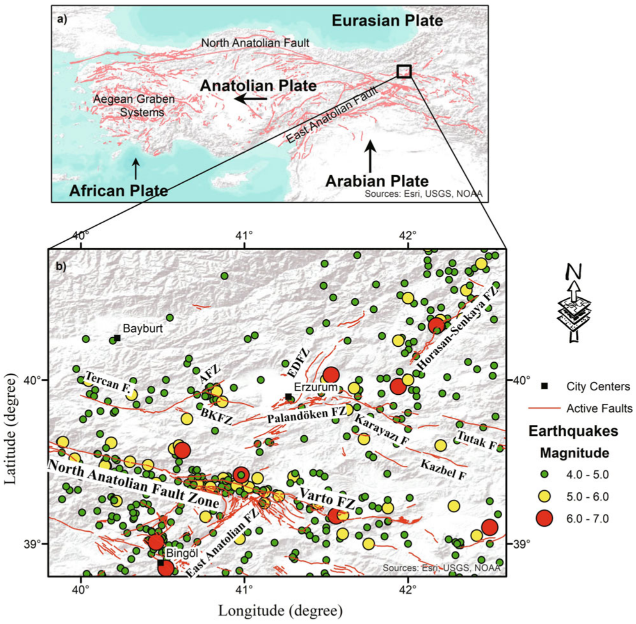

Fig. 1 (a) The tectonic plates and main tectonic features of Turkey. Arrows show the direction of tectonic plates. (b) The epicenter distribution of the earthquakes that occurred in and around Erzurum between the years 1900-2022 (AFZ: Askale fault zone, BKFZ: Baskoy-Kandilli fault zone, EDFZ: Erzurum-Dumlu fault zone. The data belonging to the earthquakes were received from https://deprem.afad.gov.tr/depremkatalogu. (The data regarding the faults were received from Emre *et al*. (2013, 2018))

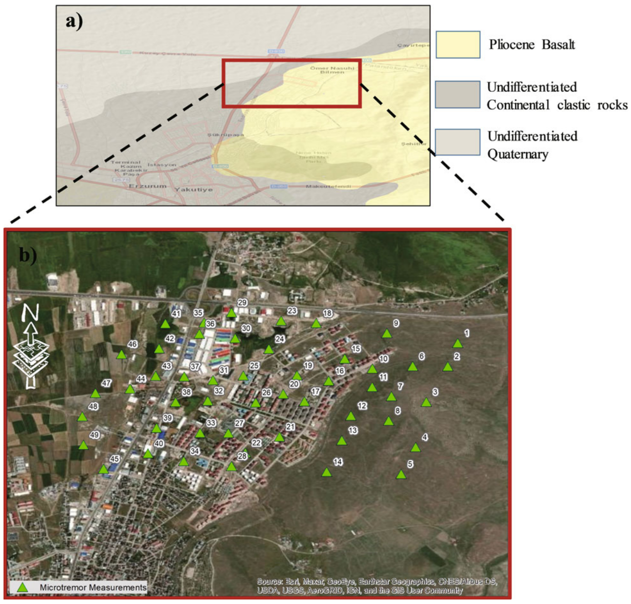

Fig. 2 (a) Simplified geological map of the study area (Akbaş *et al*., 2011; Koçyigit and Canoglu, 2017); (b) Single-station microtremor measurement locations

Table 1 The earthquakes that have affected Erzurum and its proximity since 1900 (AFAD, 2022)

Date	Longitude (degree)	Latitude (degree)	Depth (km)	Magnitude	Location
08.11.1901	41.53	40.03	10	6.1 (M_s)	Pasinler-Erzurum
28.04.1903	42.50	39.10	30	6.3 (M_s)	Malazgirt-Muş
28.12.1906	40.50	42.00	30	6.0 (M_s)	Oltu-Erzurum
13.09.1924	41.94	39.96	10	6.8 (M_s)	Köprüköy-Erzurum
17.08.1949	40.62	39.57	40	6.7 (M_s)	Tercan-Erzincan
19.08.1966	41.56	39.17	26	6.9 (M_s)	Varto-Muş
20.08.1966	40.98	39.42	14	6.2 (M_s)	Karlıova-Bingöl
30.10.1983	42.17	40.33	15	6.6 (M_w)	Horasan-Narman Erzurum
25.03.2004	40.89	39.93	10	5.6 (M_w)	Askale-Erzurum
28.03.2004	40.83	39.95	5	5.5 (M_w)	Askale-Erzurum

are Cobandede (Erzurum) volcanite between Upper Miocene-Pliocene, older quaternary alluvium, and newer alluvium (Akbaş *et al*., 2011).

New alluviums are those that are located in the middle section of plains and river valleys and continue to develop in flat areas. They cover the flat areas at the lowest part of the study area. Old alluviums are ones that previously formed on the margins of plains. They create the middle section between the alluvial layer and Cobandede volcanite in the study area and are usually firm, large granulated (sand, gravel, block) old river sediments with occasional loose formations. Çobandede volcanite is a Pliocene-aged or younger basalt volcanitesm, which are termed Cobandede basalts (Tokel, 1965) and Kargapazarı basalts (Akkuş, 1965).

3 Data and methods

3.1 Single-station microtremor measurements

Microtremors are continuous tremors on a crust that emerge from various sources (Kanai and Tanaka, 1961). The amplitudes of these tremors range between 0.001–0.01 nm and their periods are between 0.05 s and 2 s. There are multiple factors that influence these tremors: ocean waves, wind, geothermal factors, seismic activities, earthquakes, etc. Additionally, cultural effects also influence these tremors, including man-made noises such as traffic sounds or industrial clatter.

With the microtremor method, the dominant period and soil amplification value are first calculated. Subsequently, by using these parameters together with empirical relations, it is possible to calculate values such as the V_{s30} value, bedrock depth, the vulnerability index, and elastoplastic features of ground (Ibs-Von Seht and Wohlenberg, 1999; Ghofrani and Atkinson, 2014; Nakamura, 1997, 2000, 2019; Aydin *et al*., 2022).

It is possible to research the possibility of the occurrence of resonance by using the site dominant period value calculated with the use of the microtremor method, since the dominant period created by the release developed by dynamic forces can present different, the same, or close values for types of ground and buildings. When the period value for buildings and the ground is equal, it will create a resonance and the probability that a building would incur damage would increase. For this study, conducted in the fall with the single-station microtremor method, measurements were taken at 49 different locations in an area of 4 km^2. Fall was chosen as the time to do the measurements in order to minimize the effects of natural and man-made noises. In the case of ongoing construction work in areas with minimal wind and man-made noises, times during which construction equipment was not operational, were accounted for. The duration of the measurement was increased in cases in which it was not possible to minimize the effects of traffic and other noises. A Guralp CMG-6TD seismometer, a battery, a laptop, and a GPS device were utilized for the microtremor measurements. The microtremor records were measured for 30–45 minutes in the study area, with a sampling range of 100 Hz.

3.2 The horizontal to vertical spectral ratio method (Nakamura method)

This method is designed to proportion the mean square root of the Fourier amplitude spectrums of the horizontal components of the three component records, as calculated by the single-station microtremor measurement to the vertical component Fourier amplitude spectrums. Nakamura (1989) stated that microtremors are created by Rayleigh waves, which are influenced by vertical and horizontal movements at the same rate in layered subsurfaces. With this method it is assumed that vertical components are not influenced by layers of ground; however, horizontal components are influenced by low-speed layers and density. Therefore, in order to achieve the soil transfer function, the spectrums of the records of the horizontal components are proportioned to the spectrums of the vertical components.

To transform two horizontal components recorded as N-S ($NS(w)$) and E-W ($EW(w)$) into a single component, formula (1) is used and by proportioning the vertical component to $V_S(w)$, the horizontal-vertical spectral ratio mentioned in formula (2) is achieved:

$$H_S(w) = \sqrt{NS(w)^2 + EW(w)^2} \tag{1}$$

$$\frac{H}{V(w)} = \frac{H_S(w)}{V_S(w)} \tag{2}$$

Today, the single-station microtremor method is one of the most commonly used methods to identify the soil dominant period. The dominant period and the amplification factor for the locations where the measurements were taken were calculated by using the Nakamura (1989) method. The greatest advantage of this method is that it can be applied easily and swiftly inside cities or in places where there is no bedrock. Additionally, it is easy to take measurements using this method, as it does not require any reference points. The data were stored by use of the Scream 4.6 program and these data were evaluated by utilizing the GEOPSY (Wathelet *et al*., 2020) program in consideration of the SESAME (2004) criteria and the dynamic soil properties (the soil dominant period, amplification factor) as calculated and displayed in Fig. 3. While the data were evaluated by using the microtremor method in this study, a 5% cosine taper was applied to data processing phases with a band-pass filter (0.05–20 Hz). A time window length of at least 25 s was employed. Konno-Ohmachi smoothing was applied by identifying the *b* coefficient as 40 for the calculated spectrums (Konno and Ohmachi, 1998).

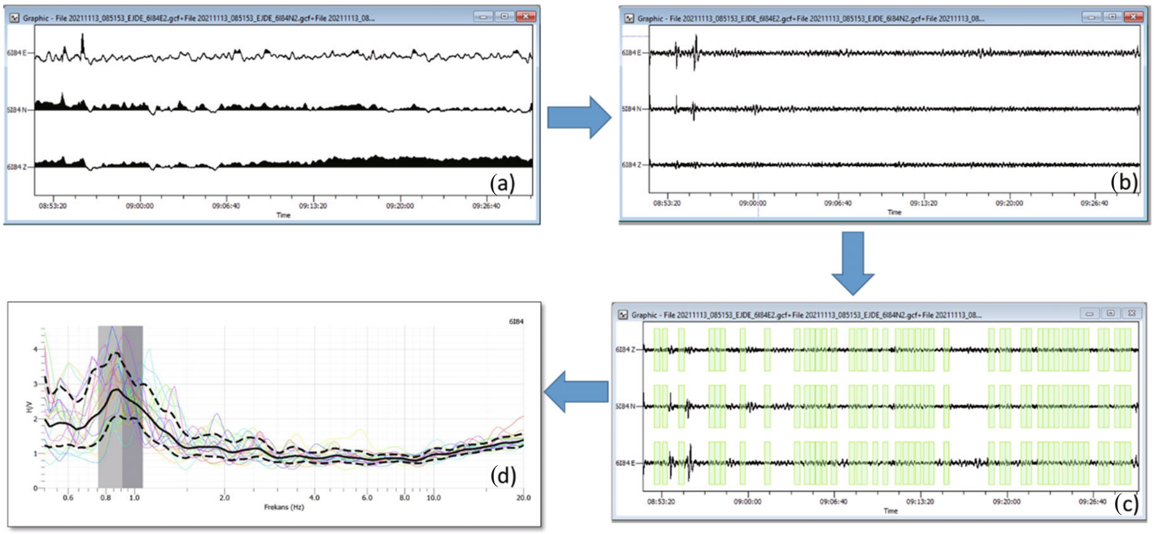

Fig. 3 Calculating the soil dominant period and the amplification factor values with the Nakamura method by using microtremor data acquired from the site: (a) raw data; (b) filtered data; (c) determination of applied time windows; (d) calculating the dominant period and the amplification factor by using the horizontal/vertical spectral ratio method

3.3 The vulnerability index (K_g)

In his studies, Nakamura (1997, 2000), by evaluating the relationship between the vulnerability index and peak amplitude and frequency, stated that by using this method it is possible to identify the hazardous zones in a study area prior to the occurrence of an earthquake. He calculated the vulnerability index (K_g) as follows:

$$K_g = A^2 \cdot T \tag{3}$$

In this equation, K_g is the vulnerability index, whereas A is the amplification factor and T is the dominant period ($1/f$) value.

3.4 Shear strain distribution

Identifying the shear strain for regions with higher earthquake hazards is crucial in mitigating earthquake damage. According to Nakamura (1996, 1997, 2000), it is possible to calculate shear strains (γ_e) using the vulnerability index (K_g), the shear wave velocity of the bedrock (V_b), and the peak ground acceleration of the bedrock, which can be calculated as follows:

$$\gamma_e = K_g \cdot \frac{e}{(\pi^2 \cdot V_b)} \cdot a_{max} \tag{4}$$

In this equation, "a_{max}" is the peak ground acceleration that can occur as a result of an earthquake. The e coefficient, which defines the activity of the strong ground motion, is assumed to be 60%, according to Nakamura (2000).

As the Turkey Earthquake Hazard Map (AFAD, 2018) reports, the peak ground acceleration for the study area with a return period of 475 years is approximately 0.45 g and is approximately 0.80 g with a return period of 2,475 years. Therefore, we calculated the shear strain value for three different scenarios by assigning the a_{max} in Eq. (4) as 0.25, 0.50 and 0.75.

Ishihara (1996) states that ground behavior changes between elastic and plastic according to the shear strain value. While ground with a shear strain value of 10^{-6}–10^{-4} have elastic features, ground with a shear strain value of 10^{-4}–10^{-2} have elastoplastic features, and ground with a shear strain value of 10^{-2}–1 demonstrate collapse features (Ishihara, 1996).

3.5 V_{s30} and frequency correlation

Ghofrani and Atkinson (2014), by using the data take from the NGA-West 2 strong ground motion database (http://peer.berkely.edu), obtained a correlation between V_{s30} and the H/V peak amplitude as well as the dominant period and developed the following equation:

$$\log_{10}(V_{s30}) = 2.8(\pm 0.02) + 0.16(\pm 0.02) \cdot (\log(f)) - 0.50(\pm 0.03)\log(A) \tag{5}$$

4 Results and discussion

As a result of evaluating the single-station microtremor measurements taken at 49 locations in the study area, site dominant frequency and the soil amplification factor were calculated by using the Nakamura method (Table 2). The frequency values corresponding to the peak amplitude in shown in HV graphs are identified as the soil dominant frequency

(Fig. 4). The foundation of the HVSR method rests on the impedance difference between soft sediment and bedrock (Elbshbeshi *et al*., 2022).

In addition to employing the *H*/*V* spectral method, the *V*/*H* spectral ratio method also is used to determine local soil effects. The *V*/*H* ratio from noise recordings is often used in oil and gas reservoir areas (Saenger *et al*., 2007; Nguyen *et al*., 2008; Pascarizativa *et al*., 2021). *V*/*H* from earthquake records is generally used in ground motion prediction equations utilizing earthquake records (Campbell, 1997; Kalkan and Gülkan, 2004; Bozorgnia and Campbell, 2016; Mazloom and Assi, 2022). In this

Table 2 Soil dominant frequency (*f*), the soil amplification factor (*H*/*V*), the vulnerability index (K_g), the soil dominant period (*T*) and the V_{s30} values formeasurement points

Measurement No.	*f* (Hz)	*H*/*V*	K_g	*T* (s)	V_{s30} (m/s)
1	1.42	1.69	2.01417	0.7052	513
2	2.18	2.08	1.98459	0.4587	495
3	2.17	2.61	3.13922	0.4608	442
4	1.44	4.27	12.66174	0.6944	323
5	1.1	4.9	21.82727	0.9091	289
6	1.02	3.35	11.00245	0.9804	345
7	1.97	2.42	2.97279	0.5076	452
8	0.8	7	61.25	1.25	230
9	0.94	5.63	33.72011	1.0638	263
10	1.78	1.9	2.02809	0.5618	501
11	1.44	2.14	3.18028	0.6944	457
12	0.89	5.25	30.9691	1.1236	270
13	5.88	1.46	0.36252	0.1701	693
14	1.44	6.49	29.25007	0.6944	262
15	17.5	1.42	0.11522	0.0571	837
16	5.61	1.04	0.1928	0.1783	815
17	4.32	1.12	0.29037	0.2315	753
18	15.3	3.66	0.87553	0.0654	510
19	0.72	4.56	28.88	1.3889	280
20	1.02	4.51	19.94127	0.9804	298
21	6.6	3	1.36364	0.1515	492
22	1.36	3.53	9.16243	0.7353	352
23	2.46	5.4	11.85366	0.4065	313
24	8.3	5.96	4.27971	0.1205	362
25	10.7	2.83	0.7485	0.0935	548
26	17.3	1.5	0.13006	0.0578	812
27	6.97	1.79	0.4597	0.1435	643
28	1.02	1.83	3.28324	0.9804	467
29	0.95	6.72	47.53516	1.0526	241
30	2.67	5.13	9.85652	0.3745	325
31	4.12	5.36	6.9732	0.2427	341
32	4.08	7.23	12.81199	0.2451	293
33	8.0	5.82	4.23405	0.125	364
34	1.1	2.06	3.85782	0.9091	446
35	0.98	5.89	35.4001	1.0204	259
36	1.36	4.4	14.23529	0.7353	315
37	1.68	7.89	37.05482	0.5952	244
38	1.8	9.08	45.80356	0.5556	230
39	1.52	4.66	14.28658	0.6579	312
40	1.76	4.97	14.0346	0.5682	309
41	2.9	2.71	2.53245	0.3448	454
42	0.93	7.95	67.95968	1.0753	221
43	1.09	7.39	50.10284	0.9174	235
44	1.06	4.68	20.66264	0.9434	294
45	0.73	5.53	41.89164	1.3699	255
46	0.7	4.72	31.82629	1.4286	274
47	0.68	5.25	40.53309	1.4706	258
48	0.83	2.49	7.47	1.2048	388
49	0.78	4.8	29.53846	1.2821	276

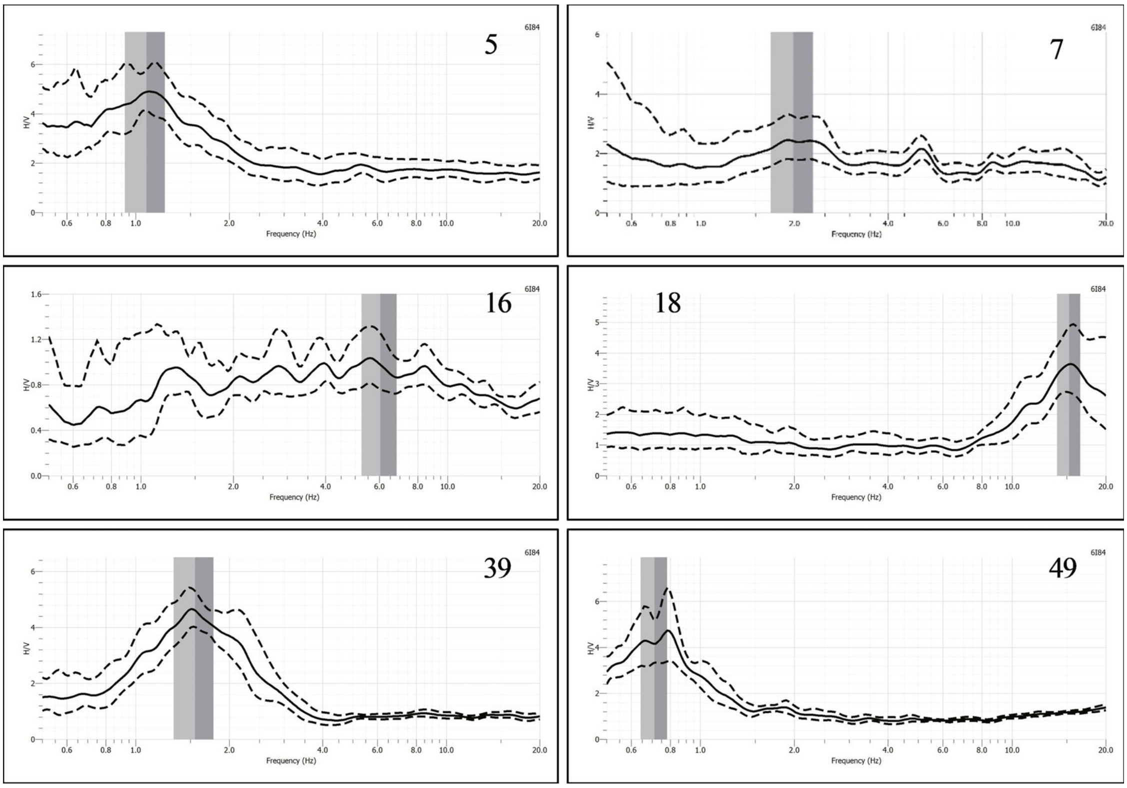

Fig. 4 Some examples of HV graphs

study, *V*/*H* ratios were analyzed for some sites (Fig. 5). It was observed that the VH ratio was generally higher at long frequencies and VH ratio values are generally lower than HV ratio values (Figs. 4 and 5).

In certain instances, this lack of contrast can be explained by the fact that the site is directly on top of bedrock, usually resulting in a linear line without any hills or pits. The spatial change in soil dominant frequency is presented in Fig. 6. The dominant frequency values vary between 0.4 Hz and 10 Hz. Lower dominant frequency values were usually observed on the alluvial ground located in the western portion of the study area. On the other hand, higher dominant frequency values were observed for the middle section of the study area. It is suggested that the lower frequency values observed in the east are related to the measurements being taken on possible bedrock.

Amplification factor values (*H*/*V*) vary between 1 and 10 (Fig. 7). While higher *H*/*V* values were observed in the western portion of the study area, lower *H*/*V* values were observed in the eastern and middle sections. The area that resulted in higher *H*/*V* values corresponds to the starting section of the Erzurum plain, which features alluvial ground (Figs. 2 and 7). Lower *H*/*V* values observed in the eastern part of the study area, however, are related to the existence of volcanite in the region. Figure 7 was developed to evaluate the *H*/*V* values together with the site dominant period values. Especially in the western portion of the study area, higher *H*/*V* values corresponding to higher period values were observed. The middle section of the study area, in which lower period values were observed and which demonstrated a higher density of buildings, provided relatively lower *H*/*V* values. It also was observed that this section had stronger ground.

The seismic vulnerability index (K_g) is one of the fundamental parameters for identifying areas that may suffer damage during an earthquake (Nakamura, 1997; Kang *et al*., 2021). Nakamura (1997) stated that there is a correlation between liquefaction and K_g. The K_g value for the study area varies between 1 and 30 (Fig. 8). Generally, lower values were observed for the middle section of the study area. Higher values (between 41 and 49) were observed for the western section of the study area, which features alluvial ground. Lower K_g values observed for the eastern section of the study area relate to volcanite. Akkaya (2020), in his study concerning the province of Van, stated that the areas with higher K_g (>10) values are directly related to buildings damaged by the 2011 Van (M_w=7.2) earthquake. Similarly, in this study it is suggested that the areas with higher K_g values are areas with higher levels of risk during an earthquake.

The shear strain for the study area was calculated by using the K_g value calculated by using the parameters measured with the Nakamura method, the shear wave velocities of the bedrock, and three different acceleration scenarios. The reason for assigning three different scenarios for the acceleration value is the fact that the Turkey Earthquake Hazard Map (AFAD, 2018) was prepared for different earthquake scenarios, and acceleration values were reported for different return periods. Therefore, in accordance with the acceleration

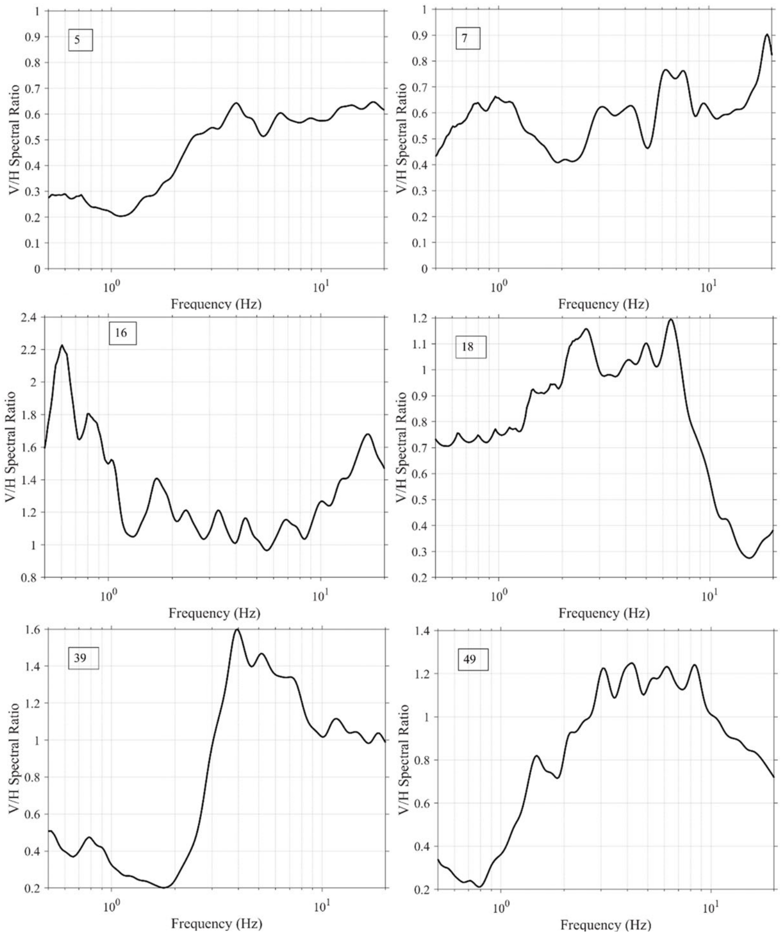

Fig. 5 Some examples of VH graphs

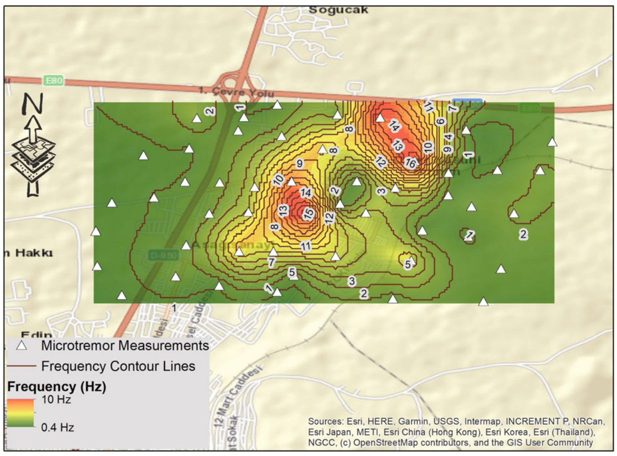

Fig. 6 The soil predominant frequency map (the white triangles show the microtremor measurement sites, and the black numbers with a gray mask represent frequency)

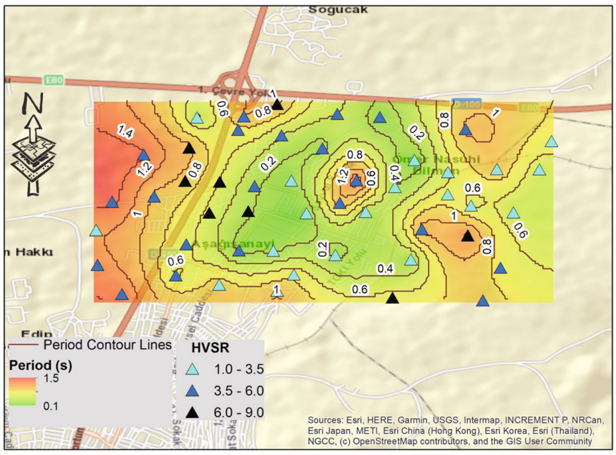

Fig. 7 The dominant period (*T*) and the soil amplification factor (HVSR) map (the triangles show the microtremor measurement sites and the black numbers with a gray mask represent the period)

values reported for the study area by AFAD, shear strain maps were created by using 0.25 g, 0.50 g and 0.75 g accelerations (Fig. 9).

While the majority of the study area presents elastoplastic features according to the shear strain map for a 0.25 g acceleration value, only the area with 42–43 measurements presented a collapse feature. Similarly, the majority of the study area presented elastoplastic features, according to the shear strain map, for a 0.50 g acceleration value. However, the number of areas with

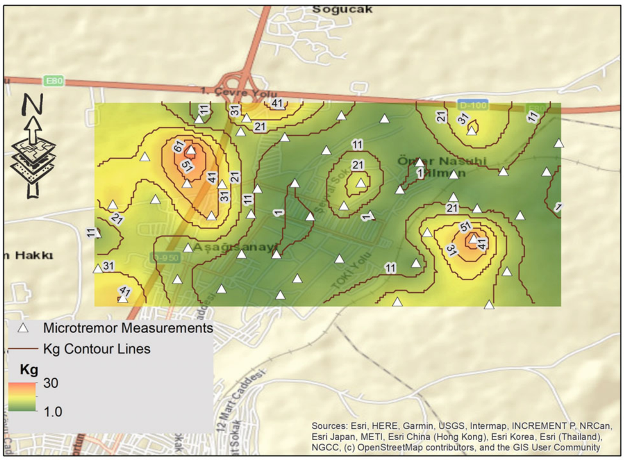

Fig. 8 The vulnerability index (K_g) map of the study area (the white triangles show the microtremor measurement sites and the black numbers with a gray mask represent K_g values)

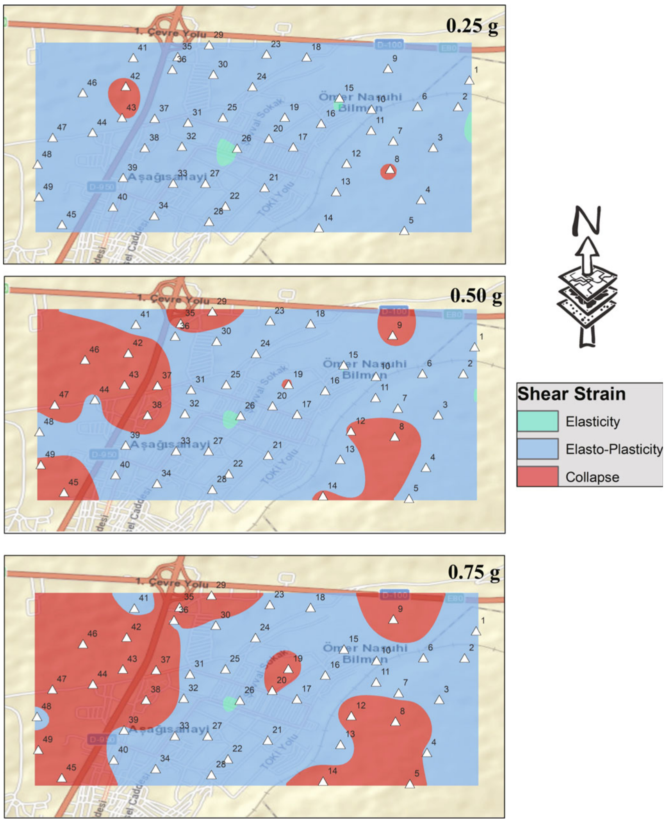

Fig. 9 The shear distribution map. The acceleration values on the bedrock are considered as 0.25 g, 0.5 g and 0.75 g

collapse behaviors increased significantly compared to the 0.25 g map. Especially in the western section of the study area, where alluvial ground is present, collapse features also were observed. It was clearly observed that the areas that presented collapse features are in correlation with areas having higher K_g (>20) values. According to the shear strain values calculated in accordance with the 0.75 g acceleration value, the middle section of the study area, where there is a greater density of buildings, presented elastoplastic features. Collapse features were observed in the western and eastern sections of the study area. As a result, it was observed that the western portion of the study area would be greatly deformed in the case of an earthquake that could produce 0.50 g or more. It is suggested that the seismic risk of this region must be investigated in great detail.

Additionally, with the empirical relation suggested by Ghofrani and Atkinson (2014), the V_{s30} value for the study area was calculated by using the frequency and the H/V value (Fig. 10). The V_{s30} values for the study area vary between 200 and 830 m/s. While lower velocity values were observed on the western part of the study area, the middle section provided higher velocity values. NEHRP (1997) and the Turkish Building Earthquake Code (TBEC, 2018) both use the same range for soil classification, according to the V_{s30} value. According to these classifications, while a large section of the study area falls into the B ($760<V_{s30}<1500$) and C ($360<V_{s30}<760$) classes, the western section was generally classified as a D ($180<V_{s30}<360$) soil class. The areas that resulted in lower V_{s30} values correspond to higher K_g values. Additionally, there were three drills and two multi channel analysis of surface wave method (MASW) conducted in the Hilalkent quarter, under the scope of the Geological-Geotechnic Study Report for Erzurum Province, Yakutiye District Building Plan (Aydıner, 2016) (Fig. 10). The V_{s30} values were calculated as 500 m/s and 460 m/s for MASW1 and MASW2, respectively. While values lower than 500 m/s were observed for the first 10 m of the MASW1 area, they increased rapidly after this depth and reached 1000 m/s at the depth of 30 m, which was considered to be in correlation with the V_{s30} calculated in this study. For the MASW2 area, values lower than 350 m/s were observed for the first 7 m and generally, values lower

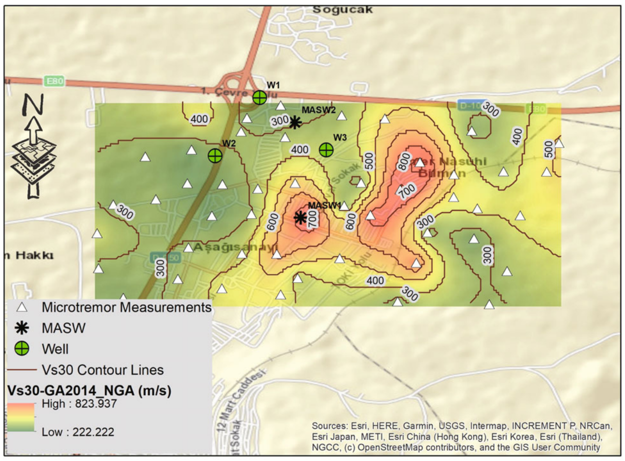

Fig. 10 The V_{s30} distribution map (the black asterisks show the MASW measurements and the green circles mark the drilling sites. The triangles show the microtremor measurement sites and the black numbers with a gray mask represent V_{s30} values)

Table 3 Equations used for calculating the amplification factor

Joyner and Fumal (1984)	Midorikawa (1987)	Borcherdt (1994)	
		Weak motion	Strong motion
$A=23\cdot V_{s30}^{-0.45}$	$A=68\cdot V_{s30}^{-0.60}$	$A=700/V_{s30}$	$A=600/V_{s30}$

than 600 m/s were observed for the first 30 m, and which was considered to be in correlation with the V_{s30} calculated in this study. Correlations between V_{s30} values and the amplification factor have been developed by different researchers (Borcherdt *et al*., 1991; Joyner and Fumal, 1984; Midorikawa, 1987). The amplification factor was calculated using these relations for the two MASW measurements in the study area (Table 3). The amplification factor values calculated using these four different equations were averaged. On average an amplification factor value of 1.4 was obtained for the MASW1 site and 1.5 for the MASW2 site. It was observed that the *H*/*V* values obtained from the microtremor measurements, especially in the area around MASW1, are compatible with the amplification factor values calculated from MASW.

The groundwater level was designated to be at approximately 5 m in the W1 well, with a depth of 15 m, and clay lithology with silted sand and small gravels was observed. In the W2 well, filling materials were observed for the first 6 m, followed by silted sand with small gravel. In the W3 well, after 2 m of slope debris, basalt lithology was observed locally. It was considered that the features identified with the microtremor method are in correlation with the soil features identified with these drills.

5 Conclusions

The purpose of this study is to identify the dynamic soil properties of the Hilalkent quarter of the Yakutiye district in Erzurum province, which has a higher risk of earthquakes, by using the single-station microtremor method. With the measurements taken for these purposes, the soil dominant period, the soil amplification factor, the V_{s30} value, the vulnerability index, and the shear strain values were calculated. While the soil dominant period and the V_{s30} values were used for soil classification, the K_g and the shear strain values were used to identify weak ground that may present damage in case of an earthquake. The soil dominant period values that were calculated as a result of evaluating microtremor measurements with the Nakamura method vary between 0.1 s and 2.5 s, and the ground amplification factor (*H*/*V*) varies between 1 and 9. Period values of >1.0 s and >3.5 *H*/*V* values were calculated for the western section of the study area. The fact that both the period and the amplification factor are higher indicates that this region has weak ground. In the middle section, where there is a greater building density, generally low period values (<1.0 s) and low *H*/*V* values (<3.5) were calculated. The V_{s30} value was calculated and mapped by using the empirical relation method. While higher V_{s30} values were observed for the middle section of the study area, other sections resulted in lower values. Upon examining them together with previously conducted drilling and MASW results, it was observed that the ground features identified with the microtremor method are in correlation with the data reported by other studies. The K_g parameter calculated by using the soil dominant period and the amplification factor indicate areas that may suffer damage during an earthquake. While higher K_g values (>10) were observed in the western section of the study area, the middle section provided lower K_g values (<10). According to the shear strain maps developed for three different bedrock accelerations, it was observed that in the case of an earthquake and an acceleration of 0.5 g or stronger, the alluvial ground in the western section of the study area may collapse and cause significant damage. As a result, while examining these parameters together, it was observed that there is a greater risk of an earthquake happening in the western section of the study area, and therefore it is suggested that this area must be opened to residency only in combination with multidisciplinary studies, and that the existing buildings must be subjected to risk evaluation.

Acknowledgment

The study includes a part of the master thesis of Fatih Karsli at the Graduate Institute of Natural and Applied Sciences in Ataturk University. We would like to thank the Ataturk University Earthquake Research Centre for the seismometer and computer support in taking microtremor measurements. We also would like to thank Geological Engineer Abdullah Ekinoglu and Geophysical Engineer MSc Omer Aydın from the Erzurum Metropolitan Municipality staff, for sharing the drilling and MASW results for the study area.

References

AFAD (2018), *Earthquake Hazard Map of Turkey*, Turkey. https://tdth.afad.gov.tr/TDTH/main.xhtml

AFAD (2022), *The Online Earthquake Catalog of Ministry of Interior Disaster and Emergency Management Presidency of Turkey*, Turkey. http://www.deprem.gov.tr

Akbaş B, Akdeniz N, Aksay A, *et al.* (2011), *1:1,250,000 Scaled Turkey Geology Map*, Maden Tetkik ve Arama Genel Müdürlüğü Yayını, Ankara-Türkiye. http://yerbilimleri.mta.gov.tr

Akbayram K, Bayrak E, Pamuk E, Özer C, Kiranşan K and Varolgüneş S (2022), "Dynamic Sub-Surface Characteristic and the Active Faults of the Genç District Locating Over the Bingöl Seismic Gap of the East Anatolian Fault Zone, Eastern Turkey," *Natural Hazards*, **114**(1): 825–847.

Akin Ö and Sayil N (2016), "Site Characterization Using Surface Wave Methods in the Arsin-Trabzon Province, NE Turkey," *Environmental Earth Sciences*, **75**(1): No. 72.

Akkaya İ (2020), "Availability of Seismic Vulnerability Index (K_g) in the Assessment of Building Damage in Van, Eastern Turkey," *Earthquake Engineering and Engineering Vibration*, **19**(1): 189–204.

Akkuş MF (1965), "Detailed Oil Survey Report of Pasinler Basin with Scale 1:25,000," *MTA Reports 4087*, USA.

Aydın U, Pamuk E and Ozer C (2022), "Investigation of Soil Dynamic Characteristics at Seismic Stations Using *H*/*V* Spectral Ratio Method in Marmara Region, Turkey," *Natural Hazards*, **110**: 587–606. https://doi.org/10.1007/s11069-021-04959-4

Aydıner M (2016), "The Geological-Geotechnic Study Report for Erzurum Province, Yakutiye District Building Plan," *Report*, Erzurum, Turkey.

Baltzopoulos G, Baraschino R, Chioccarelli E, Cito P, Vitale A and Iervolino I (2023), "Near-Source Ground Motion in the M7. 8 Gaziantep (Turkey) Earthquake," *Earthquake Engineering & Structural Dynamics*, **52**: 3903–3912.

Baser T, Nawaz K, Chung A, Faysal S and Numanoglu OA (2023), "Ground Movement Patterns and Shallow Foundation Performance in Iskenderun Coastline During the 2023 Kahramanmaras Earthquake Sequence," *Earthquake Engineering and Engineering Vibration*, **22**(4): 867–884. https://doi.org/10.1007/s11803-023-2205-9

Bayrak E, Ozer C and Perk S (2020), "Stress Tensor and Coulomb Analysis for Erzurum and Its Surroundings," *Turkish Journal of Earthquake Research*, **2**(1): 101–114. (in Turkish)

Bayrak Y and Bayrak E (2012), "An Evaluation of Earthquake Hazard Potential for Different Regions in Western Anatolia Using the Historical and Instrumental Earthquake Data," *Pure and Applied Geophysics*, **169**(10): 1859–1873.

Bayrak Y, Öztürk S, Çınar H, Kalafat D, Tsapanos TM, Koravos GC and Leventakis GA (2009), "Estimating Earthquake Hazard Parameters from Instrumental Data for Different Regions in and Around Turkey," *Engineering Geology*, **105**(3–4): 200–210.

Bayraktutan MS, Merefield JR, Grainger P, Evans BM, Yilmaz M and Kalkan E (1996), "Regional Gas Geochemistry in an Active Tectonic Zone, Erzurum Basin, Eastern Turkey," *Quarterly Journal of Engineering Geology and Hydrogeology*, **29**(3): 209–218.

Bektaş Ö, Ravat D, Büyüksaraç A, Bilim F and Ateş A (2007), "Regional Geothermal Characterization of East Anatolia from Aeromagnetic, Heat Flow and Gravity Data," *Pure and Applied Geophysics*, **164**: 975–998.

Binici B, Yakut A, Kadas K, Demirel O, Akpinar U, Canbolat A, Yurtseven F, Oztaskin O, Aktas S and Canbay E (2023), "Performance of RC Buildings After Kahramanmaras Earthquakes: Lessons Toward Performance Based Design," *Earthquake Engineering and Engineering Vibration*, **22**(4): 883–894. https://doi.org/10.1007/s11803-023-2206-8

Borcherdt RD (1994), "Estimates of Site-Dependent Response Spectra for Design (Methodology and Justification)," *Earthquake Spectra*, **10**(4): 617–653.

Borcherdt RD, Wentworth CM, Glassmoyer G, Fumal T, Mork P and Gibbs J (1991), "On the Observation and Predictive GIS Mapping of Ground Response in the San Francisco Bay Region, California," In: *Fourth International Conference on Seismic Zonation*, Stanford, California, USA, **3**: 545–552.

Bozorgnia Y and Campbell KW (2016), "Ground Motion Model for the Vertical-to-Horizontal (V/H) Ratios of PGA, PGV, and Response Spectra," *Earthquake Spectra*, **32**(2): 951–978.

Campbell KW (1997), "Empirical Near-Source Attenuation Relationships for Horizontal and Vertical Components of Peak Ground Acceleration, Peak Ground Velocity, and Pseudo-Absolute Acceleration Response Spectra," *Seismological Research Letters*, **68**(1): 154–179.

Chen WK, Rao G, Kang DJ, Wan ZF and Wang D (2023), "Early Report of the Source Characteristics, Ground Motions, and Casualty Estimates of the 2023 Mw 7.8 and 7.5 Turkey Earthquakes," *Journal of Earth Science*, **34**(2): 297–303.

Coban KH and Sayil N (2019), "Evaluation of Earthquake Recurrences with Different Distribution Models in Western Anatolia," *Journal of Seismology*, **23**: 1405–1422. https://doi.org/10.1007/s10950-019-09876-5

Coban KH and Sayil N (2020a), "Different Probabilistic Models for Earthquake Occurrences Along the North and East Anatolian Fault Zones," *Arabian Journal of Geosciences*, **13**: No. 971. https://doi.org/10.1007/s12517-020-05945-z

Coban KH and Sayil N (2020b), "Conditional Probabilities of Hellenic Arc Earthquakes Based on Different Distribution Models," *Pure and Applied Geophysics*, **177**: 5133–5145. https://doi.org/10.1007/s00024-020-02576-z

Elbshbeshi A, Gomaa A, Mohamed A, Othman A and Ghazala H (2022), "Seismic Hazard Evaluation by Employing Microtremor Measurements for Abu Simbel Area, Aswan, Egypt," *Journal of African Earth Sciences*, **196**: 104734.

Emre O, Duman TY, Ozalp S, Elmaci H, Olgun S and

Saroglu F (2013), *1/1,250,000 Scaled Turkey Active Fault Map*, General Directorate of Mineral Research and Exploration Special Publication, Turkey.

Emre O, Duman TY, Ozalp S, Saroglu F, Olgun S, Elmaci H and Can T (2018), "Active Fault Database of Turkey," *Bulletin of Earthquake Engineering*, **16**: 3229–3275.

Emre O, Koehler RD, Hengesh JV, Duman TY, Akyuz S, Altunel E and Barka A (2004), "Late Holocene Activity of Erzurum Fault Zone in Eastern Anatolia Turkey," In: *Geological Society of America Annual Meeting*, Denver, USA.

Erdik M, Biro YA, Onur T, Sesetyan K and Birgoren G (1999), "Assessment of Earthquake Hazard in Turkey and Neighboring," *Annales Geophysicae*, **42**(6): 1125–1138.

Field EH and Jacob KH (1995), "A Comparison and Test of Various Site-Response Estimation Techniques, Including Three that Are Not Reference-Site Dependent," *Bulletin of the Seismological Society of America*, **85**(4): 1127–1143.

Ghofrani H and Atkinson GM (2014), "Site Condition Evaluation Using Horizontal-to-Vertical Response Spectral Ratios of Earthquakes in the NGA-West 2 and Japanese Databases," *Soil Dynamics and Earthquake Engineering*, **67**: 30–43.

Ibs-von Seht M and Wohlenberg J (1999), "Microtremor Measurements Used to Map Thickness of Soft Sediments," *Bulletin of the Seismological Society of America*, **89**(1): 250–259.

Ishihara K (1996), *Soil Behaviour in Earthquake Geotechnics*, Oxford University Press, USA.

Jiang XY, Song XD, Li T and Wu KX (2023), "Moment Magnitudes of Two Large Turkish Earthquakes on February 6, 2023 from Long-Period Coda," *Earthquake Science*, **36**(2): 169–174.

Jirasakjamroonsri A, Poovarodom N and Warnitchai P (2019), "Seismic Site Characteristics of Shallow Sediments in the Bangkok Metropolitan Region, and Their Inherent Relations," *Bulletin of Engineering Geology and the Environment*, **78**: 1327–1343. https://doi.org/10.1007/s10064-017-1220-3

Joyner WB and Fumal TE (1984), "Use of Measured Shear-Wave Velocity for Predicting Geologic Site Effects on Strong Ground Motion," In: *Proceedings of 8th World Conference on Earthquake Engineering*, **3**: 777–783.

Kalkan E and Gülkan P (2004), "Site-Dependent Spectra Derived from Ground Motion Records in Turkey," *Earthquake Spectra*, **20**(4): 1111–1138.

Kanai K and Tanaka T (1961), "On Microtremors VIII," *Bulletin of the Earthquake Research Institute, University of Tokyo*, **39**: 97–114.

Kanbur MZ, Silahtar A and Aktan G (2020), "Local Site Effects Evaluation by Surface Wave and *H*/*V* Survey Methods in Senirkent (Isparta) Region, Southwestern Turkey," *Earthquake Engineering and Engineering Vibration*, **19**(2): 321–333. https://doi.org/10.1007/s11803-020-0564-z

Kang SY, Kim KH and Kim B (2021), "Assessment of Seismic Vulnerability Using the Horizontal-to-Vertical Spectral Ratio (HVSR) Method in Haenam, Korea," *Geosciences Journal*, **25**(1): 71–81.

Karabulut H, Güvercin SE, Hollingsworth J and Konca AÖ (2023), "Long Silence on the East Anatolian Fault Zone (Southern Turkey) Ends with Devastating Double Earthquakes (6 February 2023) Over a Seismic Gap: Implications for the Seismic Potential in the Eastern Mediterranean Region," *Journal of the Geological Society*, **180**(3): jps2023–021.

Kawase H, Sánchez-Sesma FJ and Matsushima S (2011), "The Optimal Use of Horizontal-to-Vertical Spectral Ratios of Earthquake Motions for Velocity Inversions Based on Diffuse-Field Theory for Plane Waves," *Bulletin of the Seismological Society of America*, **101**(5): 2001–2014.

Keskin M, Pearce JA and Mitchell J (1998), "Volcano-Stratigraphy and Geochemistry of Collision-Related Volcanism on the Erzurum-Kars Plateau, Northeastern Turkey," *Journal of Volcanology and Geothermal Research*, **85**(1–4): 355–404.

Koçyigit A and Canoglu MC (2017), "Neotectonics and Seismicity of Erzurum Pull-Apart Basin, East Turkey," *Russian Geology and Geophysics*, **58**(1): 99–122.

Konno K and Ohmachi T (1998), "Ground-Motion Characteristics Estimated from Spectral Ratio Between Horizontal and Vertical Components of Microtremor," *Bulletin of the Seismological Society of America*, **88**(1): 228–241.

Kramer SL (1996), *Geotechnical Earthquake Engineering*, Pearson Education India, India.

Lermo J and Chávez-García FJ (1993), "Site Effect Evaluation Using Spectral Ratios with Only One Station," *Bulletin of the Seismological Society of America*, **83**(5): 1574–1594.

Li SP, Wang X, Tao TY, Zhu YC, Qu XC, Li ZX, Huang JW and Song SY (2023), "Source Model of the 2023 Turkey Earthquake Sequence Imaged by Sentinel-1 and GPS Measurements: Implications for Heterogeneous Fault Behavior Along the East Anatolian Fault Zone," *Remote Sensing*, **15**(10): No. 2618.

Livaoğlu H, Şentürk E and Sertçelik F (2021), "A Comparative Study of Response and Fourier Spectral Ratios on Classifying Sites," *Pure and Applied Geophysics*, **178**: 1745–1759. https://doi.org/10.1007/s00024-021-02722-1

Mazloom S and Assi R (2022), "Estimate of V/H Spectral Acceleration Ratios for Firm Soil Sites in Eastern Canada," *Soil Dynamics and Earthquake Engineering*, **159**: 107350.

Melgar D, Taymaz T, Ganas A, Crowell BW, Öcalan T, Kahraman M, Tsironi V, Yolsal-Çevikbilen S, Valkaniotis

S, Irmak TS, Eken T, Erman C, Özkan B, Dogan AH and Altuntaş C (2023), "Sub- and Super-Shear Ruptures During the 2023 M_w 7.8 and M_w 7.6 Earthquake Doublet in SE Türkiye," *Seismica*, **2**(3): 1–10.

Midorikawa S (1987), "Prediction of Isoseismal Map in the Kanto Plain Due to Hypothetical Earthquake," *Journal of Structural Engineering*, **33**: 43–48.

Molnar S, Sirohey A, Assaf J, Bard PY, Castellaro S, Cornou C, Cox B, Guillier B, Hassani B, Kawase H, Matsushima S, Sánchez-Sesma FJ and Yong A (2022), "A Review of the Microtremor Horizontal-to-Vertical Spectral Ratio (MHVSR) Method," *Journal of Seismology*, **26**: 653–685.

Nakamura Y (1989), "A Method for Dynamic Characteristics Estimation of Subsurface Using Microtremor on the Ground Surface," *Quarterly Reports*, Railway Technical Research Institute, **30**(1): 25–33.

Nakamura Y (1996), "Real-Time Information Systems for Hazards Mitigation," In: *Proceeings of 7th World Conference on Earthquake Engineering*, Istanbul, Turkey, Paper No. 2134, **37**(3): 112–127.

Nakamura Y (1997), "Seismic Vulnerability Indices for Ground and Structures Using Microtremor," In: *Proceedings of World Congress on Railway Research*, Firenze, Italy, pp. 1–7.

Nakamura Y (2000), "Clear Identification of Fundamental Idea of Nakamura's Technique and Its Applications," In: *Proceedings of 12th World Conference on Earthquake Engineering*, Auckland, New Zealand, Paper No. 2656.

Nakamura Y (2019), "What Is the Nakamura Method?" *Seismological Research Letters*, **90**(4): 1437–1443. https://doi.org/10.1785/0220180376

NEHRP (1997), *Recommended Provisions for Seismic Regulations for New Buildings*, Federal Emergency Management Agency, Washington, D.C, USA.

Nguyen TT, Saenger EH, Schmalholz SM and Artman B (2008), "Earthquake Triggered Modifications of Microtremor Signals Above and Nearby a Hydrocarbon Reservoir in Voitsdorf, Austria," In: *70th EAGE Conference and Exhibition Incorporating SPE EUROPEC 2008*, European Association of Geoscientists & Engineers, Paper No. cp-40.

Okada H and Suto K (2003), *The Microtremor Survey Method*, Society of Exploration Geophysicists, USA.

Özer Ç (2019), "Investigation of the Local Soil Effects of Erzurum and Its Surroundings Using SSR and HVSR Methods," *DEU Journal of the Faculty of Engineering Journal of Science and Engineering*, **21**(61): 247–257.

Özer Ç, Öztürk S and Pamuk E (2022), "Tectonic and Structural Characteristics of Erzurum and Its Surroundings (Eastern Turkey): A Detailed Comparison Between Different Geophysical Parameters," *Turkish Journal of Earth Science*, **31**(1): 85–108.

Özer Ç and Ozyazicioglu M (2019), "The Local Earthquake Tomography of Erzurum (Turkey) Geothermal Area," *Earth Sciences Research Journal*, **23**(3): 209–223.

Öztürk S (2017), "Space-Time Assessing of the Earthquake Potential in Recent Years in the Eastern Anatolia Region of Turkey," *Earth Sciences Research Journal*, **21**(2): 67–75.

Pamuk E (2019), "Investigation of the Local Site Effects in the Northern Part of the Eastern Anatolian Region, Turkey," *Bollettino Di Geofisica Teorica ed Applicata*, **60**(4): 549–568.

Papazafeiropoulos G and Plevris V (2023), "Kahramanmaraş-Gaziantep, Türkiye M_w 7.8 Earthquake on 6 February 2023: Strong Ground Motion and Building Response Estimations," *Buildings*, **13**(5): No. 1194.

Pascarizativa R, Haris A and Alwi MSA (2021), "An Integrated Approach Using Microtremor Data for Field Development and Reservoir Monitoring: an Example from Betung Field, Jambi," In: *IOP Conference Series: Earth and Environmental Science*, **851**: 012048.

Paudyal YR, Yatabe R, Bhandary NP and Dahal RK (2012), "A Study of Local Amplification Effect of Soil Layers on Ground Motion in the Kathmandu Valley Using Microtremor Analysis," *Earthquake Engineering and Engineering Vibration*, **11**(2): 257–268. https://doi.org/10.1007/s11803-012-0115-3

Putti SP and Satyam N (2020), "Evaluation of Site Effects Using HVSR Microtremor Measurements in Vishakhapatnam (India)," *Earth Systems and Environment*, **4**: 439–454.

Park CB, Miller RD and Xia JH (1999), "Multichannel Analysis of Surface Waves," *Geophysics*, **64**(3): 800–808.

Saenger EH, Torres A, Rentsch S, Lambert M, Schmalholz SM and Mendez-Hernandez E (2007), "A Hydrocarbon Microtremor Survey Over a Gas Field: Identification of Seismic Attributes," In: *SEG Technical Program Expanded Abstracts 2007*, Society of Exploration Geophysicists, USA, pp. 1277–1281.

SESAME (2004), *Guidelines for the Implementation of the H/V Spectral Ratio Technique on Ambient Vibrations: Measurements, Processing and Interpretation*, SESAME European Research Project, Deliverable D23.12, Project No. EVG1-CT-2000-00026 SESAME.

Shao GL, Wen RZ, Wang HW, Ren YF and Zhou BF (2023), "Spatial Correlations in Ground Motion Intensity Measuring from 2023 Turkey Earthquake," *Earthquake Research Advances*, **4**(1): 100231.

Soysal H, Sipahioglu S, Koak D and Altinok Y (1981), "Historical Earthquake Catalogue of Turkey and Surrounding Area (2100 B.C.–1900 A.D.)," *Technical Report*, Tubitak, No. TBAG-341.

Tallini M, Lo Sardo L and Spadi M (2020), "Seismic Site Characterisation of Red Soil and Soil-Building Resonance Effects in L'Aquila Downtown (Central Italy)," *Bulletin of Engineering Geology and the Environment*, **79**: 4021–4034. https://doi.org/10.1007/s10064-020-01795-x

Tavlaşoğlu E (2021), "Geological and Geotechnical Study for Aziziye Region, Erzurum," *Master Thesis*, Ataturk University Graduate School of Natural and Applied Sciences Department of Geological Engineering, Erzurum, Turkey. (in Turkish)

TBEC (2018), *Turkish Seismic Earthquake Code*, Disaster and Energency Management Prisidency, Goverment of Republic of Turkey, Ankara, Turkey. Retrieved from https://www.resmigazete.gov.tr/eskiler/2018/03/20180318M1-2-1.pdf

Tokel S (1965), "Erzurum I16-b2 ve Tortum H46-c3 paftalarına ait jeolojik rapor," *MTA Reports*, USA.

Wang XH, Feng GC, He LJ, An Q, Xiong ZQ, Lu H, Wang WX, Li N, Zhao YG, Wang YD and Wang YX (2023), "Evaluating Urban Building Damage of 2023 Kahramanmaras, Turkey Earthquake Sequence Using SAR Change Detection," *Sensors*, **23**(14): No. 6342.

Wathelet M, Chatelain JL, Cornou C, Di Giulio G, Guillier B, Ohrnberger M and Savvaidis A (2020), "Geopsy: A User-Friendly Open-Source Tool Set for Ambient Vibration Processing," *Seismological Research Letters*, **91**(3): 1878–1889. https://doi.org/10.1785/0220190360.

Wen RZ, Ren YF and Shi DC (2011), "Improved HVSR Site Classification Method for Free-Field Strong Motion Stations Validated with Wenchuan Aftershock Recordings," *Earthquake Engineering and Engineering Vibration*, **10**(3): 325–337. https://doi.org/10.1007/s11803-011-0069-x

Xu TH, Wang WQ and Zhang ZG (2023), "Strong Ground Motion Simulations of the 2023 Turkey–Syria Earthquake Sequence Using CGFDM3D-EQR," *Copernicus Meetings*, Vienna, Australia, Paper No. EGU23-17607.

Zavala N, Clemente-Chávez A, Figueroa-Soto Á, González-Martínez M and Sawires R (2021), "Application of Horizontal to Vertical Spectral Ratio Microtremor Technique in the Analysis of Site Effects and Structural Response of Buildings in Querétaro City, Mexico," *Journal of South American Earth Sciences*, **108**: 103211.

Zhao JJ, Chen Q, Yang YH and Xu Q (2023), "Coseismic Faulting Model and Post-Seismic Surface Motion of the 2023 Turkey–Syria Earthquake Doublet Revealed by InSAR and GPS Measurements," *Remote Sensing*, **15**(13): No. 3327.